NASA TECHNICAL MEMORANDUM

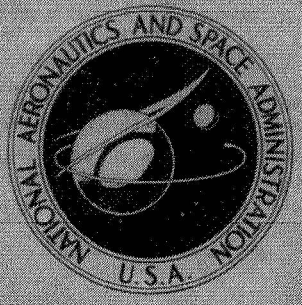

NASA TM X-1997

NASA TM X-1997

JET-PLUME-INDUCED FLOW SEPARATION ON A LIFTING ENTRY BODY AT MACH NUMBERS FROM 4.00 TO 6.00

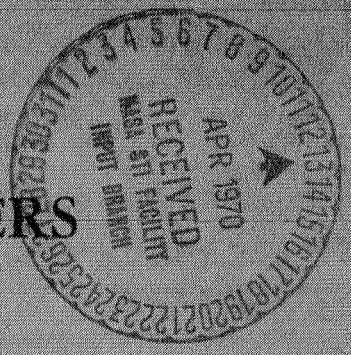

by Robert J. McGhee

Langley Research Center

Langley Station, Hampton, Va.

NATIONAL AERONAUTICS AND SPACE ADMINISTRATION • WASHINGTON, D. C. • APRIL 1970

1. Report No.	2. Government Accession No.	3. Recipient's Catalog No.
NASA TM X-1997		

4. Title and Subtitle	5. Report Date
JET-PLUME-INDUCED FLOW SEPARATION ON A LIFTING ENTRY BODY AT MACH NUMBERS FROM 4.00 TO 6.00	April 1970
	6. Performing Organization Code

7. Author(s)	8. Performing Organization Report No.
Robert J. McGhee	L-6980
	10. Work Unit No.
9. Performing Organization Name and Address	126-13-10-22-23
NASA Langley Research Center Hampton, Va. 23365	11. Contract or Grant No.
	13. Type of Report and Period Covered
12. Sponsoring Agency Name and Address	Technical Memorandum
National Aeronautics and Space Administration Washington, D.C. 20546	14. Sponsoring Agency Code

15. Supplementary Notes

16. Abstract

The investigation showed that increasing the ratio of jet-exit static pressure to free-stream static pressure resulted in plume-induced boundary-layer separation along the model lower surface and also resulted in an increase in the pressures in the separation region and a forward movement of the separation point. The pressure distributions obtained on the center line of the model showed characteristics of both laminar and transitional separation. Increasing the angle of attack resulted in a decrease in the extent of flow separation for all test Mach numbers; this result may partially be due to local Reynolds number changes. Two-dimensional laminar separation theory resulted in reasonable correlation of the plateau pressure coefficients obtained on the center line of the model.

17. Key Words (Suggested by Author(s))	18. Distribution Statement
Jet plumes Lifting body Flow separation	Unclassified – Unlimited

19. Security Classif. (of this report)	20. Security Classif. (of this page)	21. No. of Pages	22. Price*
Unclassified	Unclassified	30	$3.00

*For sale by the Clearinghouse for Federal Scientific and Technical Information
Springfield, Virginia 22151

JET-PLUME-INDUCED FLOW SEPARATION ON A LIFTING ENTRY BODY AT MACH NUMBERS FROM 4.00 TO 6.00

By Robert J. McGhee
Langley Research Center

SUMMARY

Some effects of jet-plume-induced boundary-layer separation on the flat bottom of a lifting entry model have been investigated at free-stream Mach numbers from 4.00 to 6.00 and for an angle-of-attack range from 0^{o} to 14^{o}. Schlieren data and surface pressure data were obtained for a nozzle-exhaust Mach number of 2.24. The range of the ratios of jet-exit static pressure to free-stream static pressure was from jet off to about 1400 at a free-stream Mach number of 4.00 and from jet off to about 5200 at a free-stream Mach number of 6.00. The free-stream Reynolds number per meter was approximately 3.58×10^{6} and 3.15×10^{6} at free-stream Mach numbers of 4.00 and 6.00, respectively.

The investigation showed that increasing the ratio of jet-exit static pressure to free-stream static pressure resulted in plume-induced boundary-layer separation along the model lower surface and also resulted in an increase in the pressures in the separation region and a forward movement of the separation point. The pressure distributions obtained on the center line of the model showed characteristics of both laminar and transitional separation. Increasing the angle of attack resulted in a decrease in the extent of flow separation for all test Mach numbers; this result may partially be due to local Reynolds number changes. Two-dimensional laminar separation theory resulted in reasonable correlation of the plateau pressure coefficients obtained on the center line of the model.

INTRODUCTION

An understanding of flow-separation phenomena is of importance in the design of configurations for high aerodynamic efficiency. The surface pressure distribution on a vehicle is generally altered by flow separation with resulting adverse effects on the vehicle aerodynamic forces and moments. Flight at high altitudes of rocket-powered vehicles results in the rocket-motor nozzles exhausting at pressures substantially exceeding the ambient pressure. For even moderate underexpansion, large billowing exhaust plumes result and often cause extensive boundary-layer flow separation. Serious consequences

for high-fineness-ratio lifting-entry vehicles can be anticipated if propulsive aerodynamic maneuvering is required.

The present investigation was initiated to obtain initial information on the effects of large jet plumes on boundary-layer flow separation for a lifting entry body. Surface pressure distributions and schlieren photographs were obtained for the model at Mach numbers from 4.00 to 6.00 and angles of attack from about 0° to 14°. A supersonic exhaust nozzle was used with compressed gaseous nitrogen to obtain the rocket-exhaust plume.

SYMBOLS

$C_{p,p}$ plateau pressure coefficient, $\frac{p_p - p_o}{q_o}$

l_s separation length, distance from separation point to model base based on schlieren measurements

L total model length, 24.69 cm

M Mach number

p static pressure

q dynamic pressure

$R_{x,o}$ Reynolds number at beginning of pressure interaction, $\frac{\rho_o V_o x_o}{\mu_o}$

V velocity

x longitudinal coordinate

α angle of attack

μ coefficient of viscosity

ρ mass density of air

Subscripts:

j jet-exit conditions, calculated from ideal one-dimensional nozzle flow

o condition at beginning of interaction

p condition in region of pressure plateau

∞ free-stream condition

APPARATUS AND TESTS

Model

A general arrangement of the model, sting, and nozzle assembly is shown in figure 1 and details of the model and supersonic nozzle are presented in figures 2 and 3, respectively. The model was constructed of fiber glass with an inner steel core to provide for sting mounting. The model had a delta planform and a triangular cross section with a flat bottom surface. The leading-edge sweep angle was 80° and the angle between the sides and the bottom surface was 45°. All edges and the nose leading edge had a radius of about 0.04 cm. The ratio of length to maximum span of the configuration was 2.78.

The model support sting, a hollow steel tube, allowed the gaseous nitrogen from the supply tank to be emptied through louvers (fig. 1) into a settling chamber ahead of the nozzle. The supersonic nozzle was designed as an annular nozzle because of the presence of the center support sting and because only the outer plume boundary needed to be simulated. For this investigation, the inner structure of the plume is believed to be inconsequential. Allowance was made in the nozzle design for the presence of the center support sting. The area ratio of the nozzle was 2.07 and the exit Mach number for one-dimensional isentropic flow was calculated to be 2.24. Cold gaseous nitrogen at approximately local atmospheric total temperature was used to obtain the exhaust plume.

Wind Tunnel

The tests were conducted in a 2-foot hypersonic facility at the Langley Research Center. This wind tunnel, described in reference 1, is an ejector-type facility which provides continuous flow at high Mach numbers and low densities. The average test conditions for the present investigation are shown in the following table:

M_{∞}	Stagnation temperature, $^{\circ}K$	Stagnation pressure, kN/m^2	Static pressure, kN/m^2	Reynolds number per meter
4.00	356	101	0.69	3.58×10^6
4.50	422	137	.54	2.79
5.00	422	179	.37	3.18
6.00	422	278	.17	3.15

Nitrogen Supply

High pressure gaseous nitrogen was generated by pumping liquid nitrogen to the required storage pressure and converting it from a liquid to a gas in a steam-actuated heat exchanger. The high-pressure gaseous nitrogen was then stored in a tank farm with a capacity of 22.65 m^3. Suitable pressure-reducing and pressure-regulated valves were remotely controlled to obtain the nitrogen gas pressure in a manifold outside the test section which, in turn, fed the nozzle plenum chamber in the model. Once the correct pressure was obtained in the manifold, a quick-acting guillotine valve was employed to initiate and terminate the flow to the nozzles. Minor pressure adjustments could be made after initiation of flow through the nozzles.

Instrumentation

Ten static pressure orifices (0.15 cm in diameter) were located on the center line of the flat bottom on the model as shown in figure 2. Simultaneous measurements of the local pressures as well as the nozzle plenum pressure were obtained from absolute-pressure-measuring transducers. Data were obtained by a high-speed data acquisition system and recorded on magnetic tapes. In addition, schlieren photographs were taken at each datum point with the use of a 2-microsecond flash from a xenon light source.

Tests and Accuracy

The model was tested at free-stream Mach numbers from 4.00 to 6.00. For the supersonic nozzle employed, p_j/p_∞ varied from jet off to about 1400 at $M_\infty = 4.00$ and from jet off to about 5200 at $M_\infty = 6.00$. The model angle of attack was adjusted to obtain data from about 0^o to 14^o. All data were obtained with the model smooth; that is, no boundary-layer transition strips were used. At the Reynolds numbers of these tests, laminar flow was considered to exist over the entire model at jet-off conditions.

The ratios of p_j/p_∞ and p/p_∞ quoted herein are estimated to be accurate within ±2 percent. The Mach number in the region of the test model was accurate within ±0.04. Angle-of-attack values are estimated to be accurate within $\pm 0.1^o$.

RESULTS AND DISCUSSION

Surface-pressure data for the model are presented in figure 4 and schlieren photographs in figure 5 to illustrate the effects of jet pressure ratio, Mach number, and angle of attack. The effect of free-stream Mach number on the surface-pressure data for a constant jet pressure ratio is shown in figure 6; whereas its effect on the length of the separation region is shown in figure 7. Comparison of the model local pressures at jet-off conditions with theory of reference 2 is shown in figure 8. Comparison of the plateau

pressure coefficients from the present investigation with results from other sources and with theory are presented in figure 9, and the trends with local Mach number for a constant jet pressure ratio are compared in figure 10. References 3 to 7 illustrate both experimental and theoretical separated flow results induced by solid surfaces.

Experimental Results

Effect of jet pressure ratio.- The schlieren photographs of figure 5(a) $\left(M_\infty = 6.00, \alpha = 0^o\right)$ show that the flow separates over the model lower surface as the jet pressure ratio is increased. As the size of the jet plume is increased $\left(\text{as } p_j/p_\infty \text{ is increased}\right)$, the separated flow region moves forward on the model lower surface. At a jet pressure ratio of $p_j/p_\infty = 4637$, about 70 percent of the lower surface is shown to be in a region of separated flow. The corresponding pressure distribution on the model lower surface in the separated flow region is shown in figure 4(a). These pressure distributions have been compared with those of references 4 and 5 which are typical of boundary-layer separation induced by a solid surface. For the lower values of p_j/p_∞ and hence smaller regions of flow separation, the present data are characteristic of laminar separation without a plateau. As the plume size increases, the pressure distributions are characteristic of laminar separation with a pressure plateau. Finally, at the highest values of p_j/p_∞, the data display an additional pressure rise following a plateau similar to that observed in references 4 and 5 which has been termed transitional separation. The present data exhibit no pressure profiles typical of turbulent separation at $\alpha = 0^o$.

Effect of Mach number.- Figure 4(a) indicates that at $\alpha = 0^o$, decreasing the free-stream Mach number results in a reduction in the pressure rise from the beginning of the interaction to the pressure plateau, and the schlieren photographs of figure 5(f) show that the length of flow separation is reduced. This effect is better illustrated in figure 6 where the pressure distributions are shown for all four test Mach numbers at a constant jet pressure ratio of $p_j/p_\infty \approx 1300$. Measured values from schlieren photographs of the nondimensionalized length of flow separation l_s/L along the model lower surface at $\alpha = 0^o$ are shown for all four test Mach numbers in figure 7. The flow was assumed to separate from the lower surface of the model directly below the intersection of the outer edge of the boundary layer and the shock wave generated by the separation region. When plotted in this way, the data appear to exhibit two different characteristic variations with p_j/p_∞ at all free-stream Mach numbers. At the lower values of p_j/p_∞, the length of flow separation increases rapidly, at about the same slope for all test Mach numbers. Additional increases in p_j/p_∞ result in a rapid decrease in the slope of the curve for l_s/L plotted against p_j/p_∞. This rapid change in slope suggests that it may be associated with the change from laminar to transitional separation as discussed previously.

Effect of angle of attack.- Figures 4(b) to 4(e) illustrate the effect of angle of attack on the local pressure distribution and the schlieren photographs of figure 5 illustrate the corresponding flow fields. Increasing the angle of attack to 2° showed small effects on the pressure distribution or flow field at $M_{\infty} = 6.00$. Angles of attack greater than 2° showed a reduction in the extent of flow separation for all Mach numbers. For example, at $\alpha = 10^{\circ}$, figure 4(d) indicates only about 10 percent of the body is subject to any pressure change as a result of jet pluming. The schlieren photographs also clearly indicate this decrease in flow separation. (See figs. 5(d) and 5(h).) However, increasing the angle of attack changes the local Reynolds number and thus the location of transition. The observed decrease in the extent of separation may partially result from a change in separation characteristics due to changes in local Reynolds number. Therefore, the observed decrease in the extent of separation is not necessarily a true angle-of-attack effect.

Comparison With Theory

Viscous-interaction theory.- The pressure distribution on a sharp-edge flat plate is a result of the displacement effect of the plate boundary layer on the external flow. Several theoretical methods are available for predicting the pressure distributions on a sharp-edge flat plate which account for boundary-layer growth. The experimental pressure distribution for the model of the present investigation at $M_{\infty} = 6.00$, jet-off conditions, and $\alpha = 0^{\circ}$ is compared with the second-order weak interaction theory for a sharp-edge flat plate of reference 2 (for a Prandtl number of 0.725) in figure 8. The theory agrees closely with the present experimental data.

Correlation of plateau-pressure coefficients.- The investigation of references 4 and 7 have indicated that laminar separation phenomena are strongly dependent on the local flow conditons at the beginning of the interaction leading to separation. In figure 9, the correlation curves of references 4 and 7 relating the variation of $C_{p,p}(R_{x,o})^{1/4}$ with M_o are shown. Also shown in the figure are the results of the present test for a wide range of jet pressure ratio at $\alpha = 0^{\circ}$ along with the results of references 3 to 6. It should be noted that the two lowest points for the data of the present investigation are for pressure ratios of 342 and 529, where the plateau pressure (fig. 4(a)) is well defined; whereas, at the higher values of p_j/p_{∞}, the plateau pressures were obtained for transitional separation. References 4 and 5 have indicated that plateau data for transitional separation can be correlated with laminar separation if transition occurs sufficiently close to reattachment. Most of the data points for various jet pressure ratios fall between the semiempirical curves. In figure 10, the variation of $C_{p,p}(R_{x,o})^{1/4}$ with M_o for a constant jet pressure ratio of $p_j/p_{\infty} \approx 1300$ is shown. The magnitude of $C_{p,p}(R_{x,o})^{1/4}$ for the three values of M_o fall between the two semiempirical curves.

CONCLUDING REMARKS

An investigation has been conducted in the 2-foot hypersonic facility at the Langley Research Center to determine the effects of jet-plume-induced boundary-layer flow separation on the flat bottom of a lifting entry model. The tests were conducted at free-stream Mach numbers from 4.00 to 6.00 and an angle-of-attack range from 0° to 14°.

As the size of the jet plume is increased by increasing the jet-pressure ratio, the separated-flow region moves forward on the body and the pressures in the separated region increase. The pressure distributions obtained on the center line of the model showed characteristics of both laminar and transitional separation. Increasing the angle of attack decreased the extent of flow separation for all test Mach numbers; this decrease may partially result from a change in separation characteristics due to local Reynolds number changes. Two-dimensional laminar separation theory resulted in reasonable correlation of the plateau-pressure coefficients obtained on the center line of the model.

Langley Research Center,
National Aeronautics and Space Administration,
Langley Station, Hampton, Va., January 28, 1970.

REFERENCES

1. Stokes, George M.: Description of a 2-Foot Hypersonic Facility at the Langley Research Center. NASA TN D-939, 1961.

2. Hayes, Wallace D.; and Probstein, Ronald F.: Hypersonic Flow Theory. Academic Press, Inc., 1959.

3. Townsend, James C.: Effects of Leading-Edge Bluntness and Ramp Deflection Angle on Laminar Boundary-Layer Separation in Hypersonic Flow. NASA TN D-3290, 1966.

4. Chapman, Dean R.; Kuehn, Donald M.; and Larson, Howard K.: Investigation of Separated Flows in Supersonic and Subsonic Streams With Emphasis on the Effect of Transition. NACA Rep. 1356, 1958. (Supersedes NACA TN 3869.)

5. Sterrett, James R.; and Emery, James C.: Extension of Boundary-Layer Separation Criteria to a Mach Number of 6.5 by Utilizing Flat Plates With Forward-Facing Steps. NASA TN D-618, 1960.

6. Putnam, Lawrence E.: Investigation of Effects of Ramp Span and Deflection Angle on Laminar Boundary-Layer Separation at Mach 10.03. NASA TN D-2833, 1965.

7. Erdos, John; and Pallone, Adrian: Shock-Boundary Layer Interaction and Flow Separation. RAD-TR-61-23 (Contract AF04(647)-685), AVCO Corp., Aug. 15, 1961.

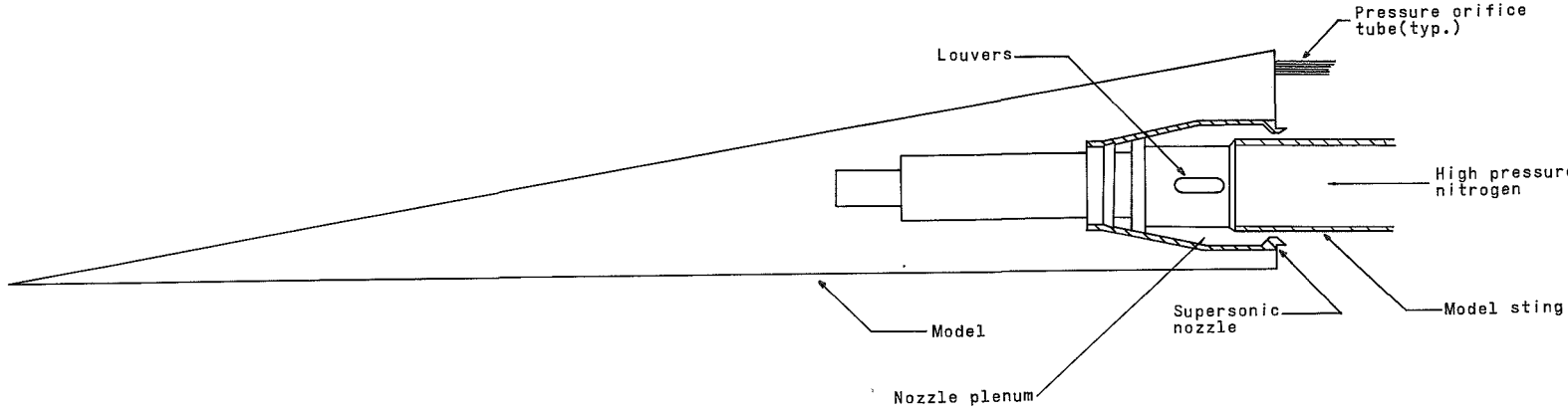

Figure 1.- Sketch of model showing sting and nozzle arrangement.

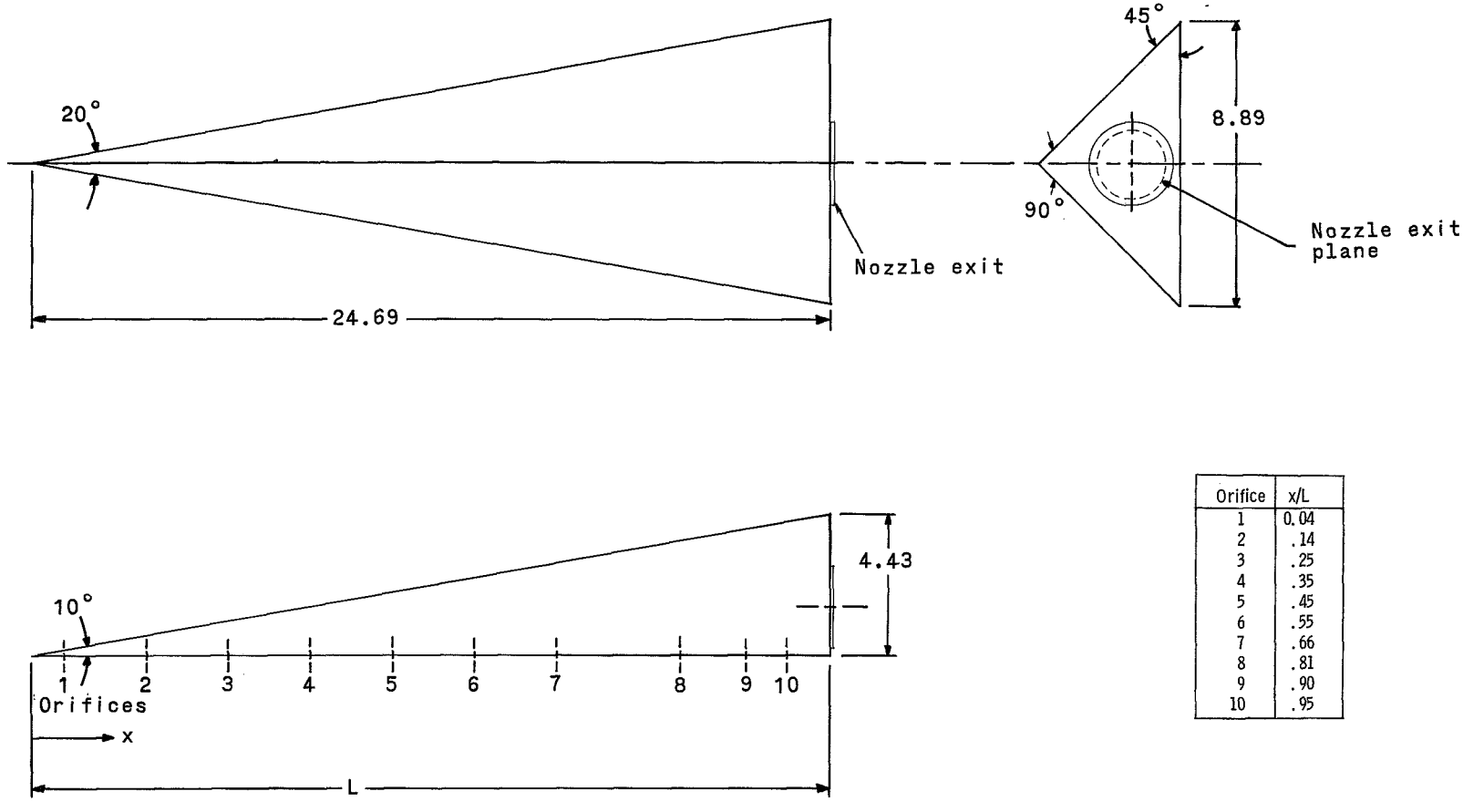

Orifice	x/L
1	0.04
2	.14
3	.25
4	.35
5	.45
6	.55
7	.66
8	.81
9	.90
10	.95

Figure 2.- Model drawing. All linear dimensions are given in centimeters.

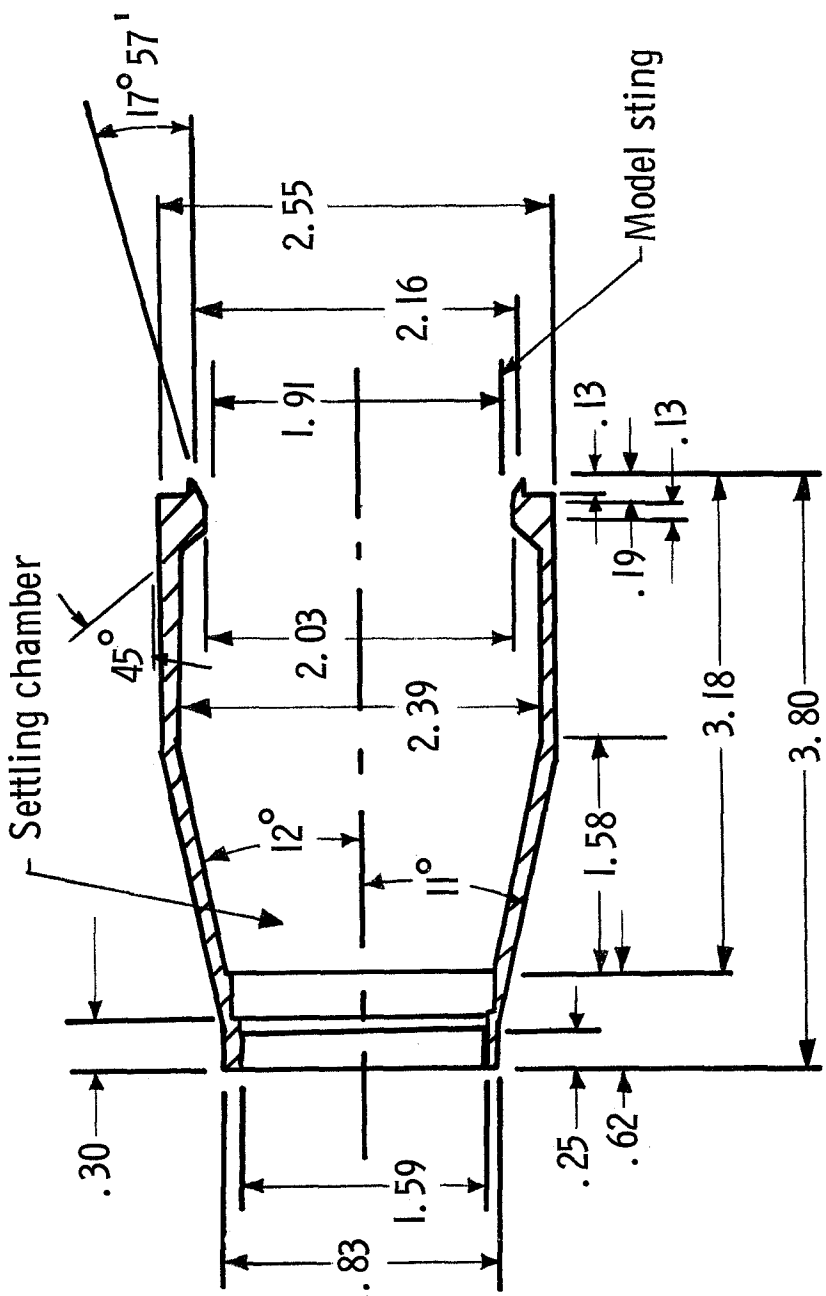

Figure 3.- Details of supersonic nozzle. All linear dimensions are given in centimeters.

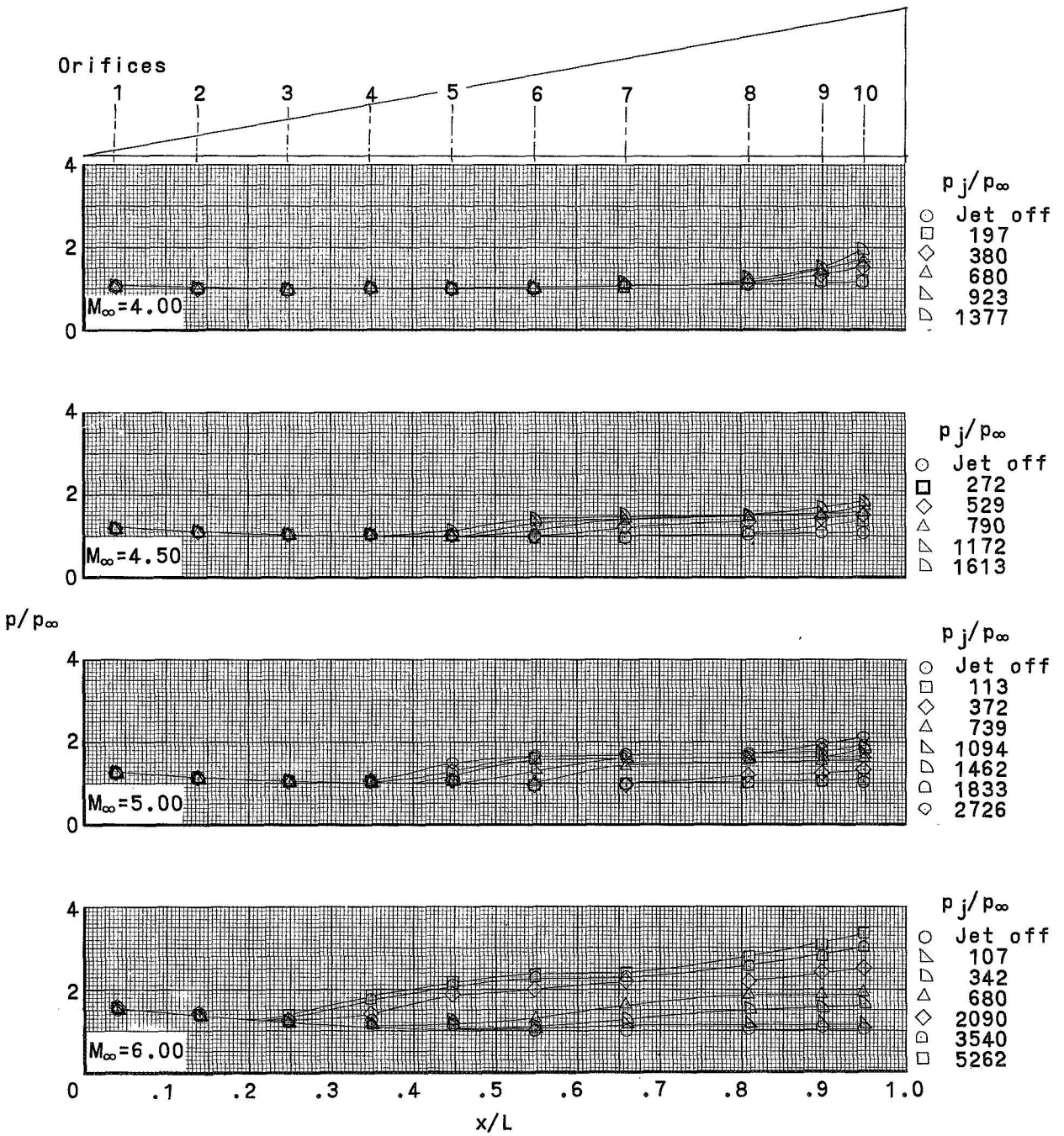

(a) $\alpha = 0^{o}$.

Figure 4.- Effect of jet pressure ratio and Mach number on the model pressure distribution.

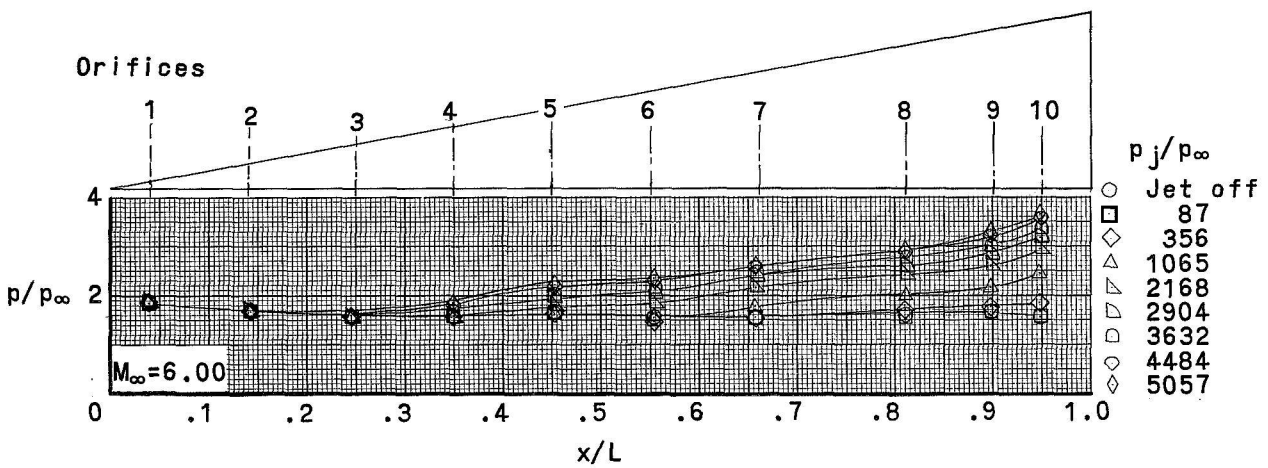

(b) $\alpha = 2^{0}$.

Figure 4.- Continued.

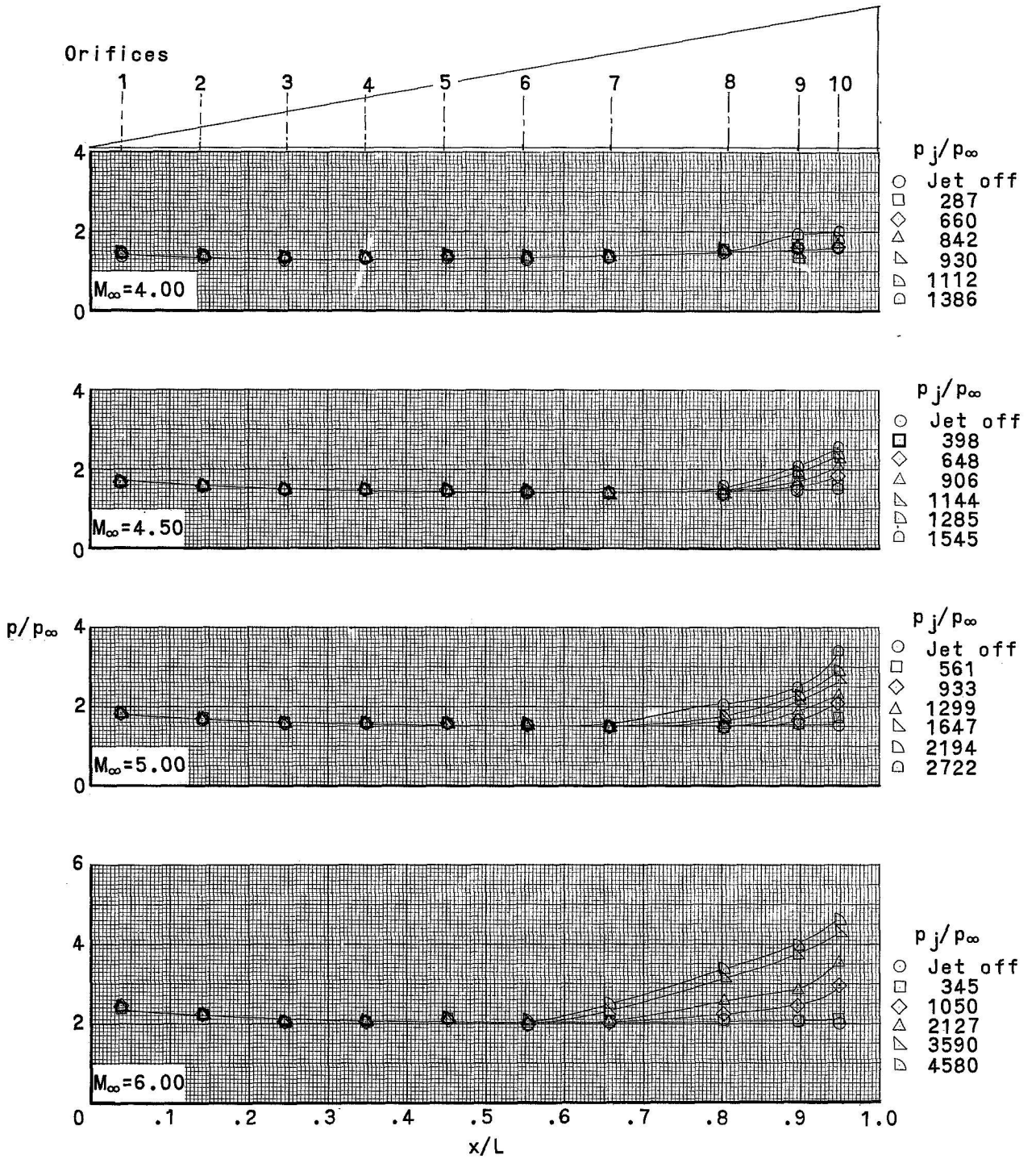

(c) $\alpha = 5^0$.

Figure 4.- Continued.

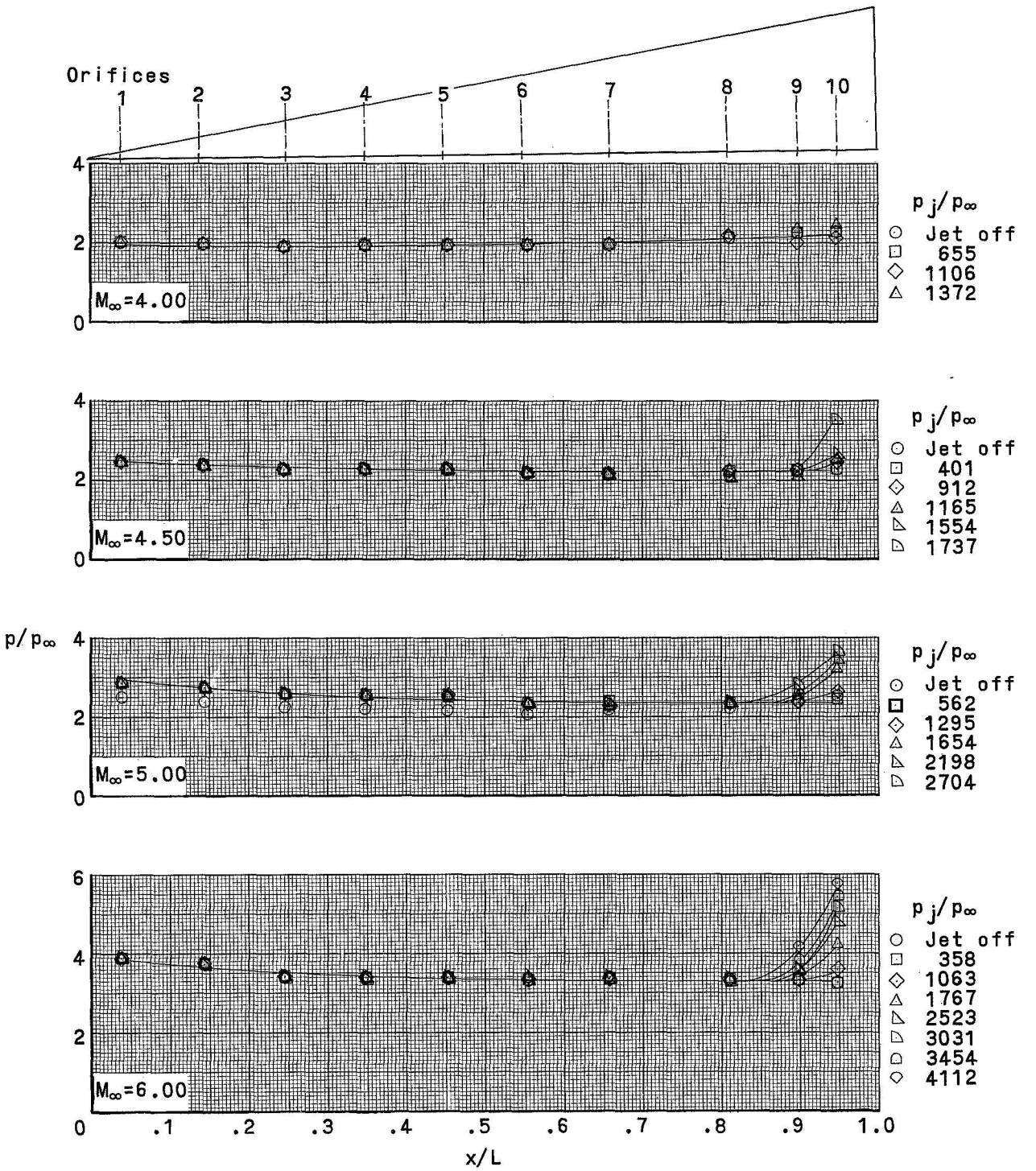

(d) $\alpha = 10^{0}$.

Figure 4.- Continued.

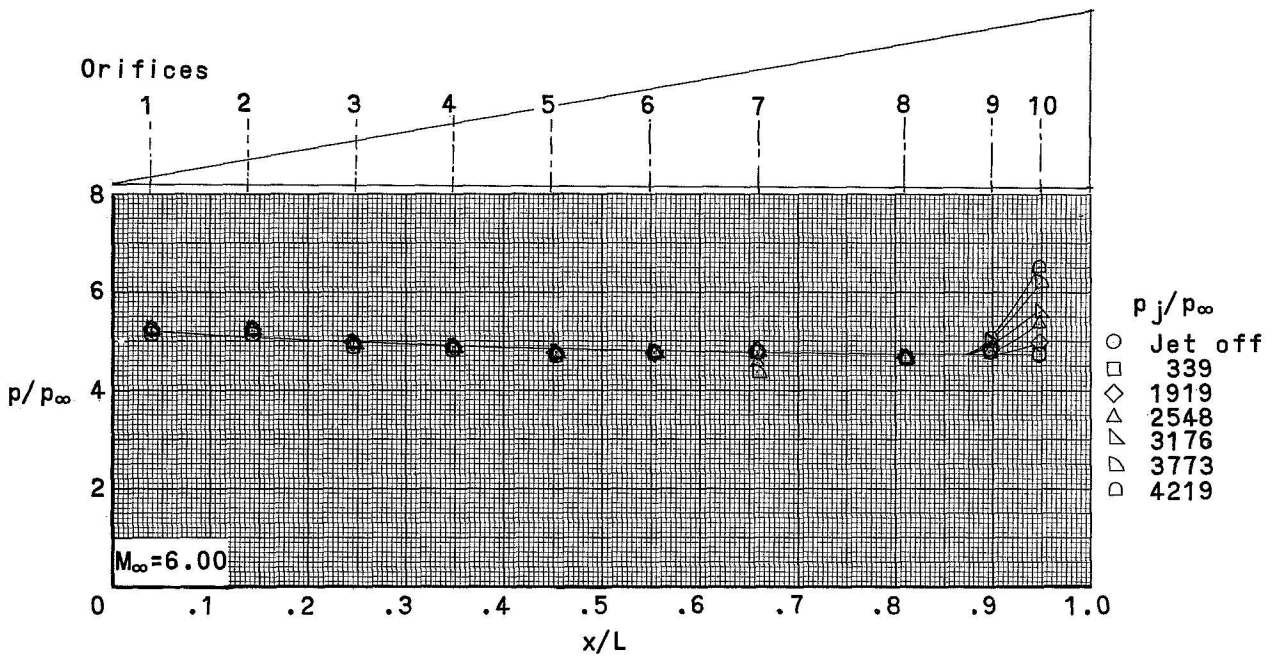

(e) $\alpha = 14^{0}$.

Figure 4.- Concluded.

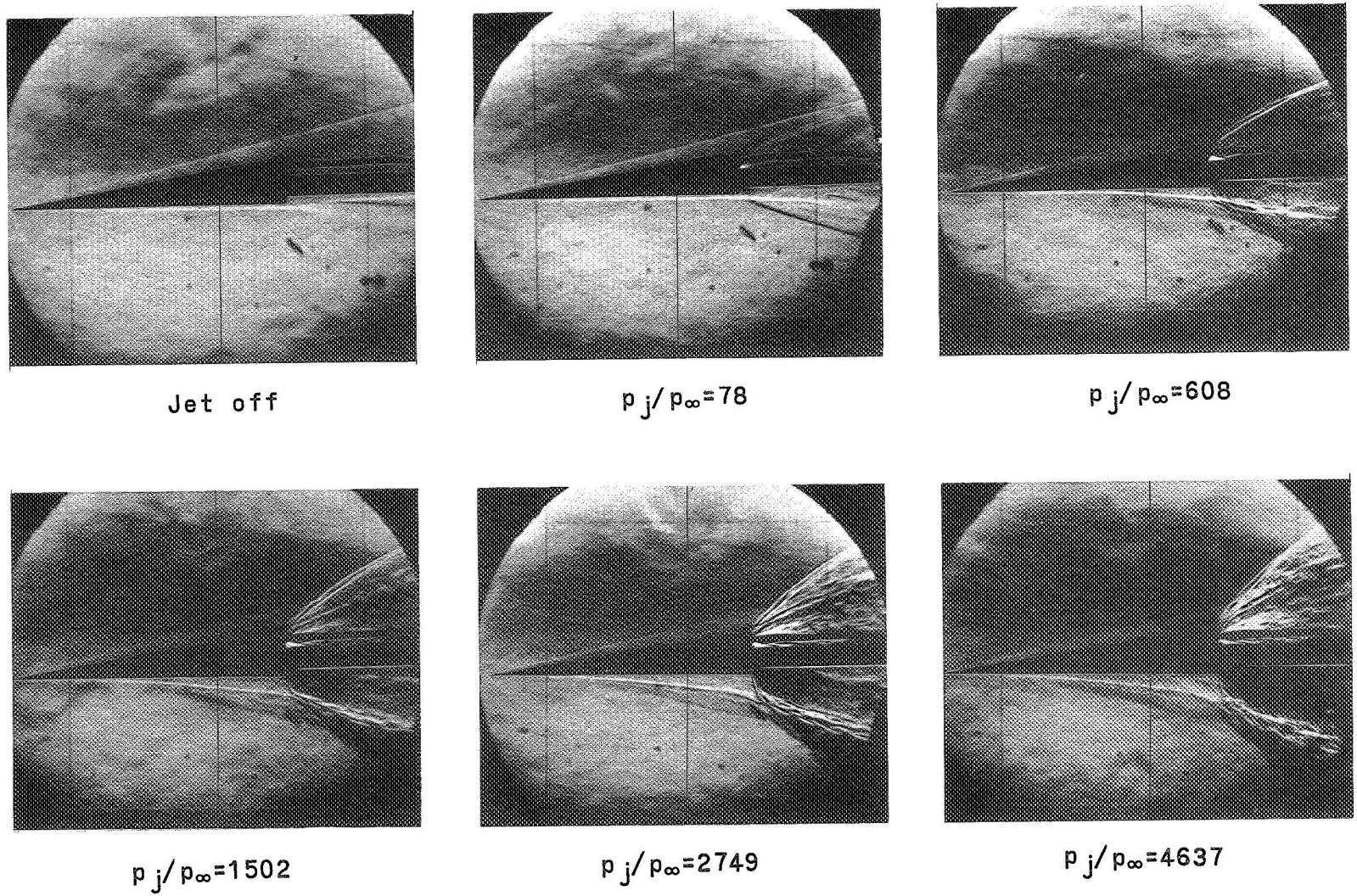

L-70-1513

(a) $M_\infty = 6.00$; $\alpha = 0^0$.

Figure 5. Representative schlieren photographs showing the effect of jet pressure ratio on the flow over the model.

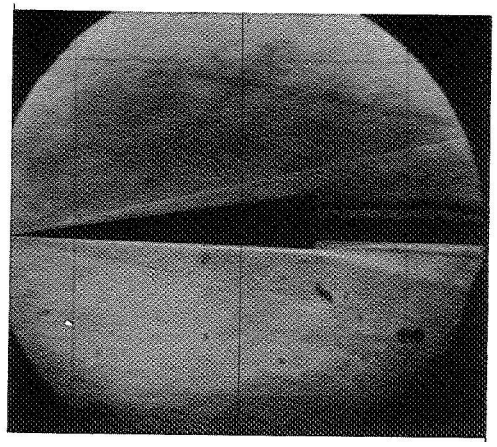

Jet off

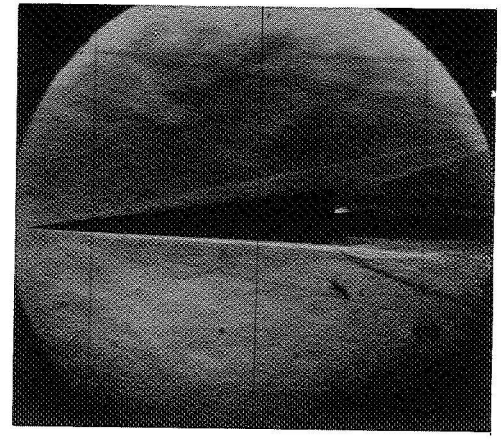

p_j/p_∞=89

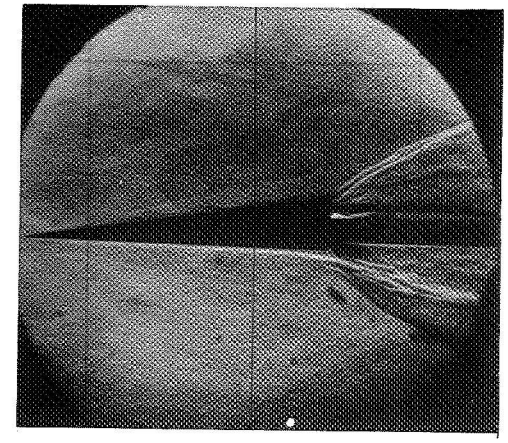

p_j/p_∞=898

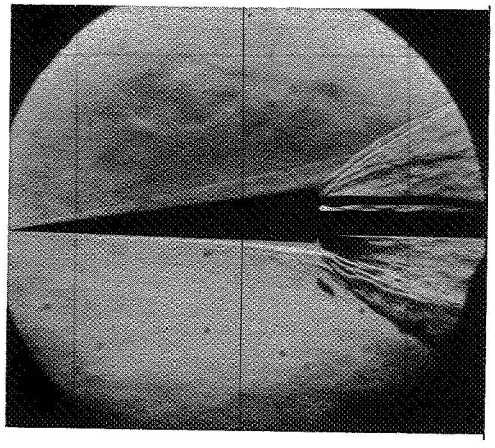

p_j/p_∞=1480

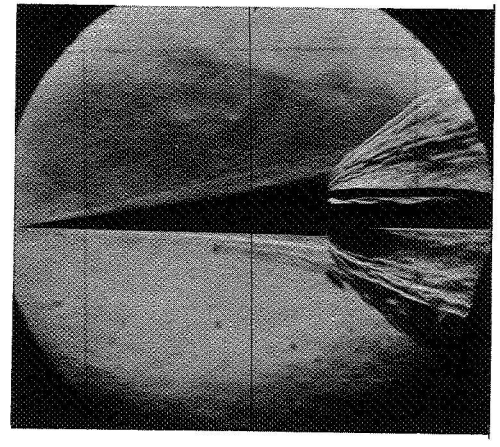

p_j/p_∞=2721

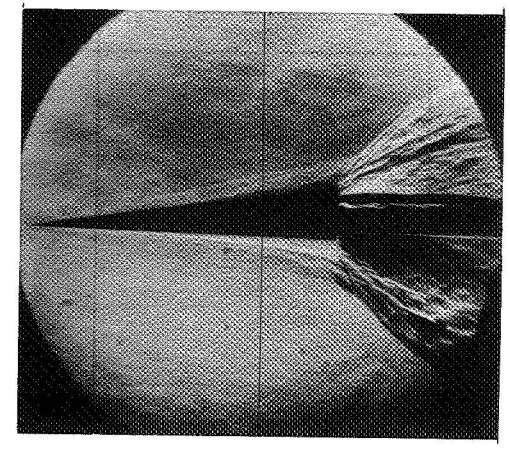

p_j/p_∞=4528

(b) $M_\infty = 6.00$; $\alpha = 2^0$.

L-70-1514

Figure 5.- Continued.

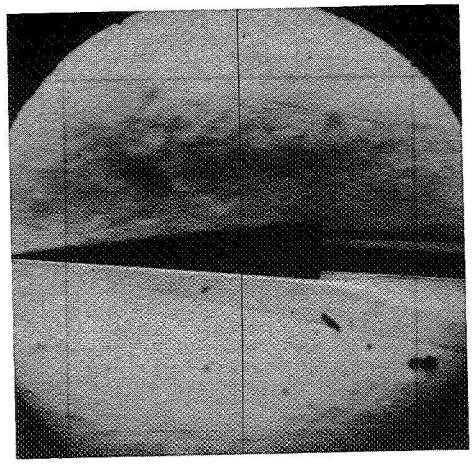

Jet off

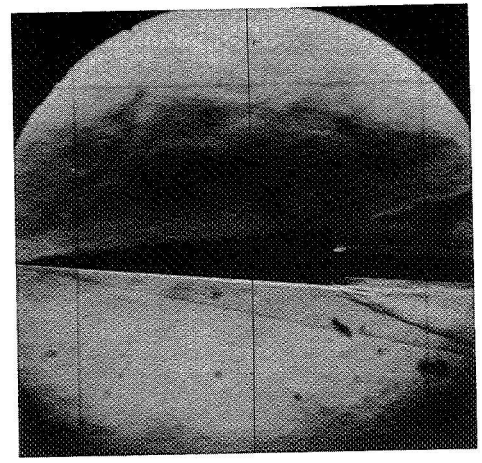

p_j/p_∞=72

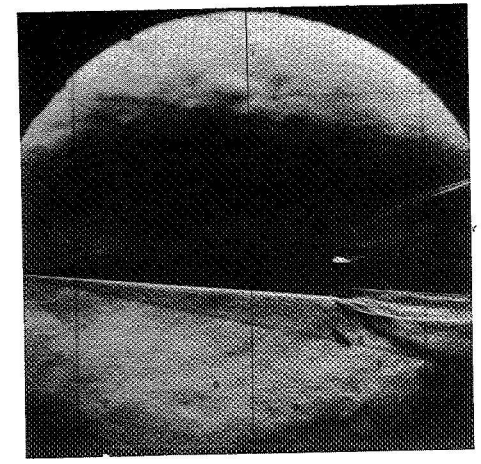

p_j/p_∞=285

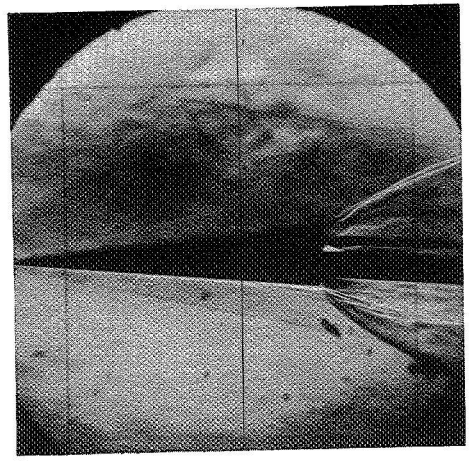

p_j/p_∞=621

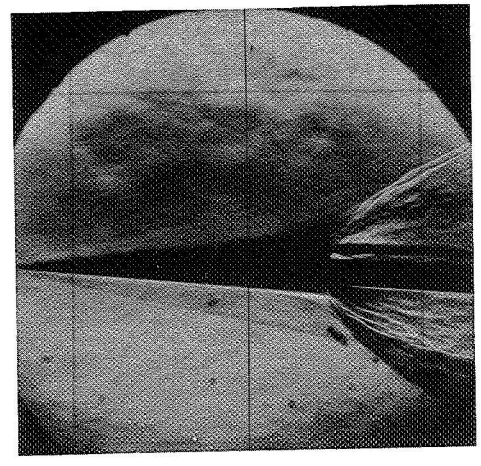

p_j/p_∞=1522

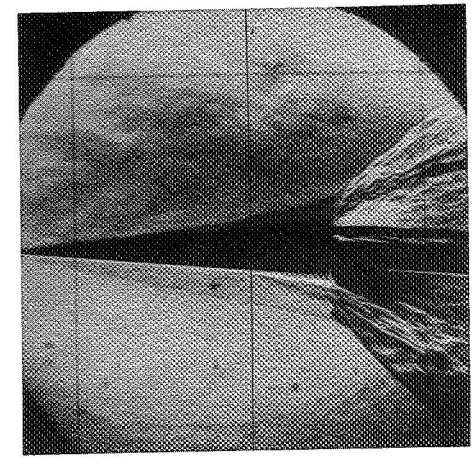

p_j/p_∞=4569

L-70-1515

(c) $M_\infty = 6.00$; $\alpha = 5^0$.

Figure 5.- Continued.

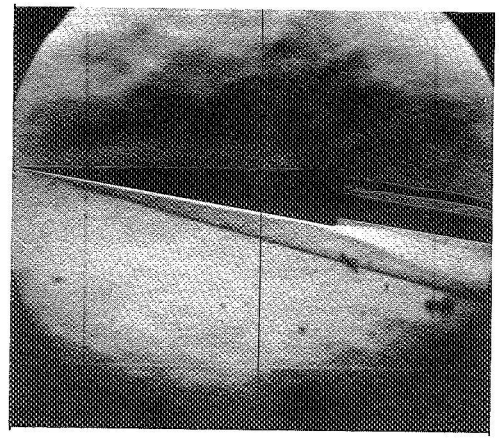

Jet off

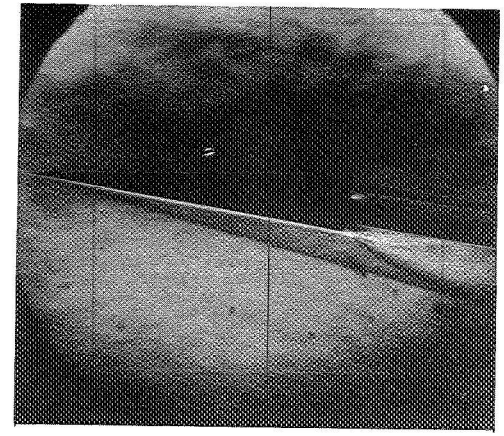

p_j/p_∞=90

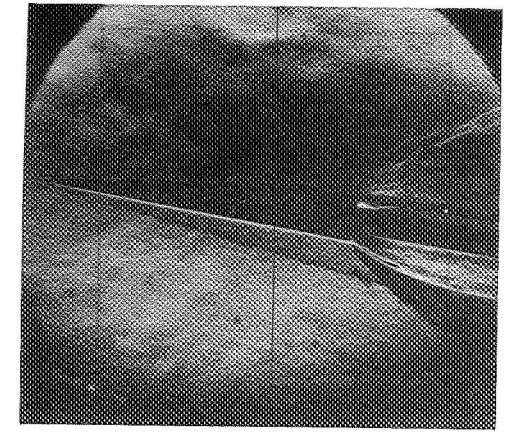

p_j/p_∞=893

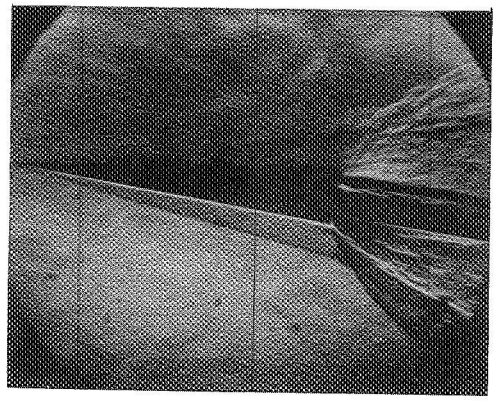

p_j/p_∞=2780

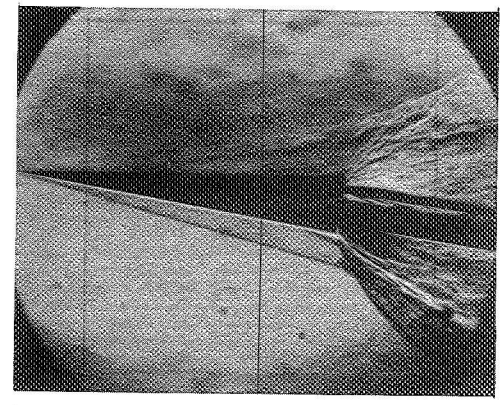

p_j/p_∞=3109

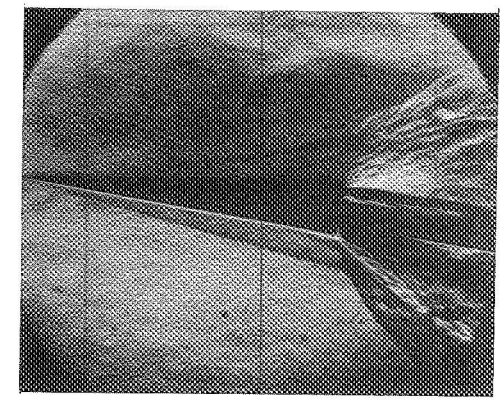

p_j/p_∞=4604

(d) $M_\infty = 6.00$; $\alpha = 10^0$.

L-70-1516

Figure 5.- Continued.

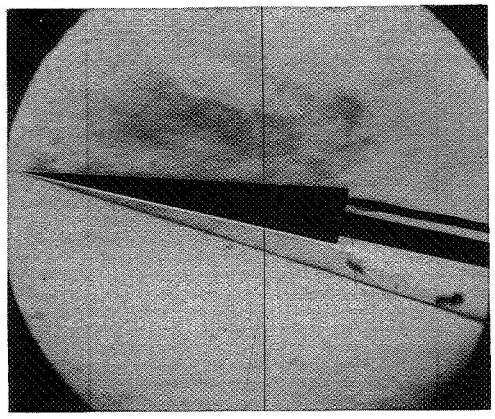

Jet off

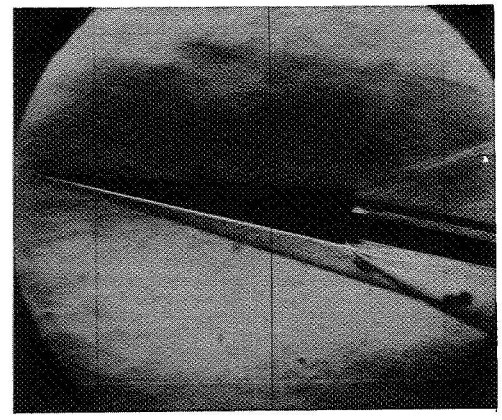

p_j/p_∞=189

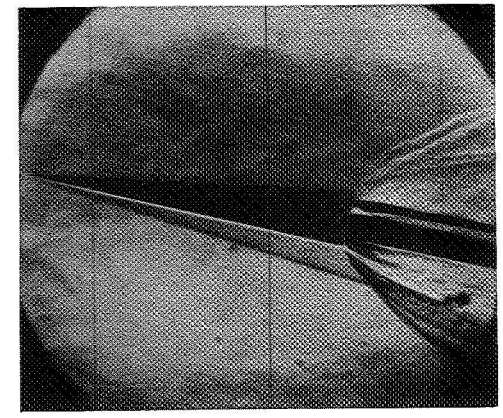

p_j/p_∞=1287

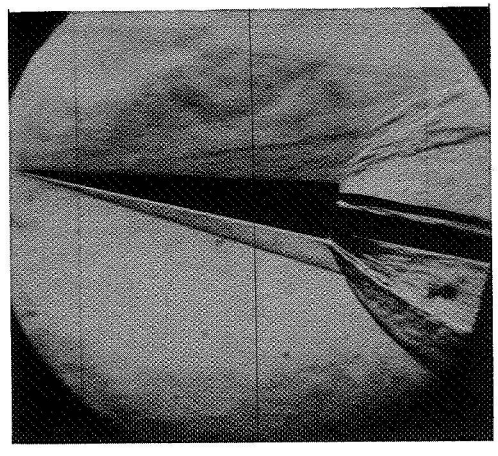

p_j/p_∞=2864

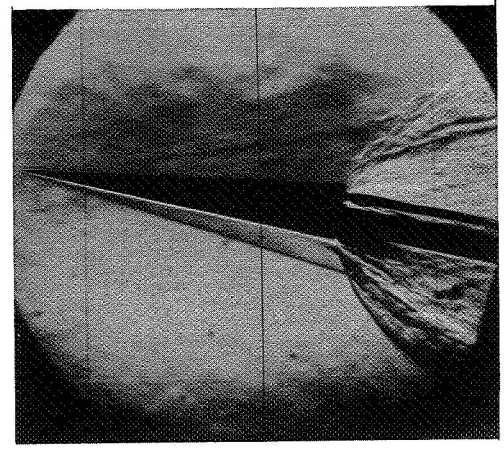

p_j/p_∞=3773

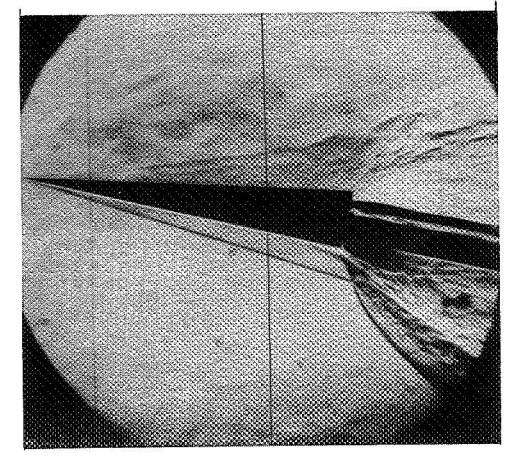

p_j/p_∞=4219

(e) $M_\infty = 6.00$; $\alpha = 14^0$.

L-70-1517

Figure 5.- Continued.

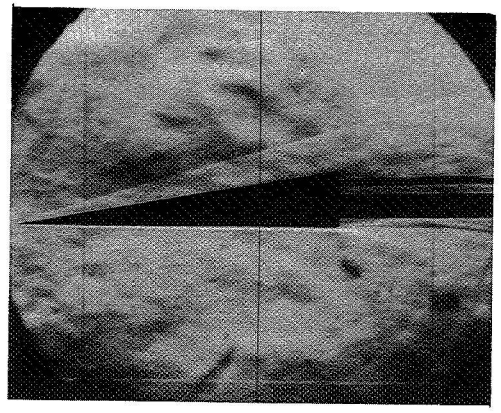

Jet off

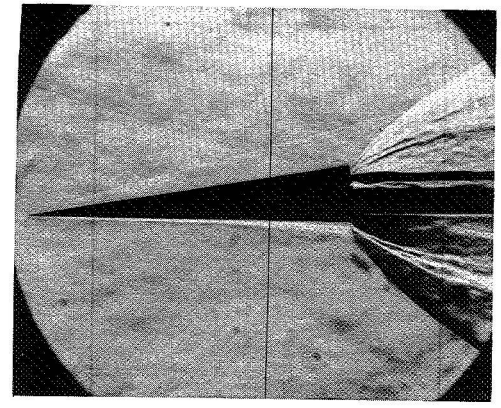

p_j/p_∞=923

M_∞=4.00

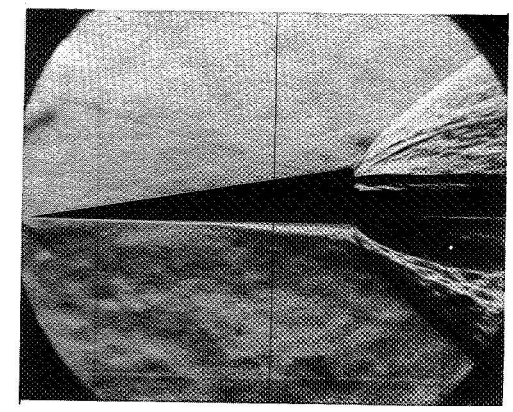

p_j/p_∞=1377

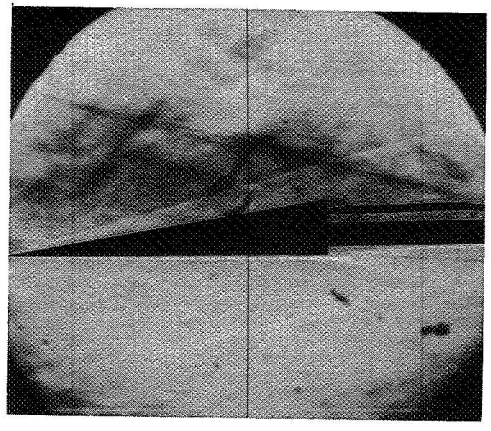

Jet off

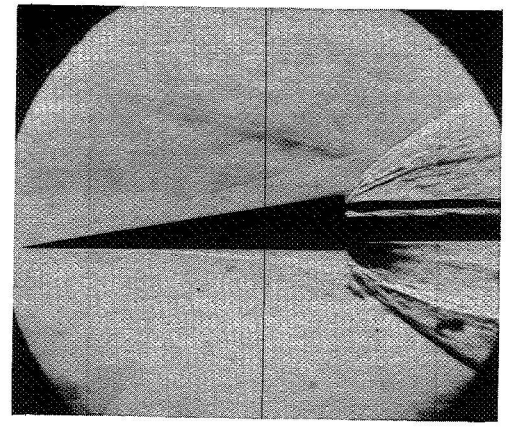

p_j/p_∞=1044

M_∞=4.50

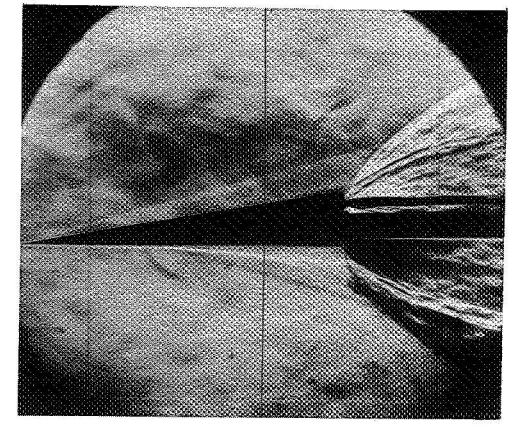

p_j/p_∞=1614

(f) M_∞ = 4.00 and 4.50; α = 0°.

L-70-1518

Figure 5.- Continued.

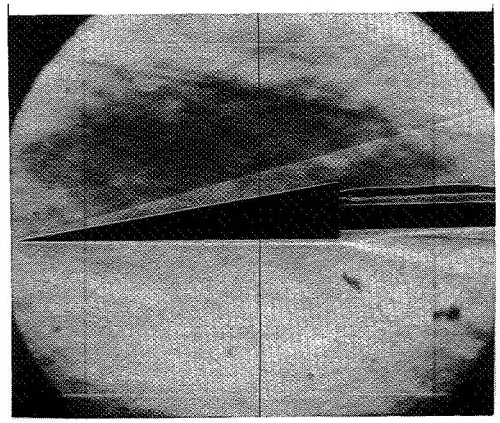

Jet off

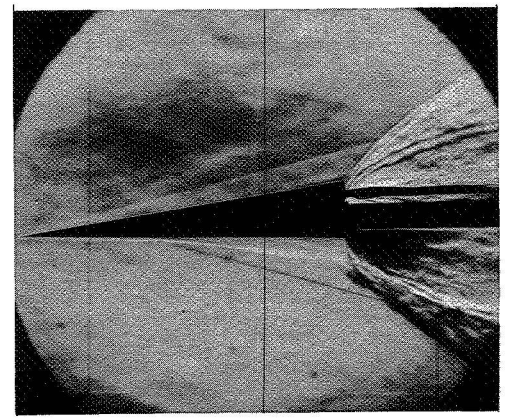

$p_j/p_\infty=1834$

$M_\infty=5.00$

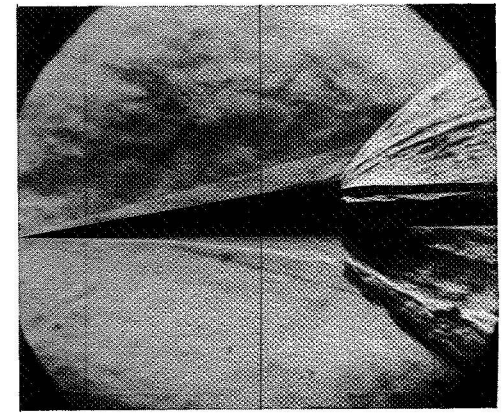

$p_j/p_\infty=2727$

(f) $M_\infty = 5.00$; $\alpha = 0^0$. Concluded.

L-70-1521

Figure 5.- Continued.

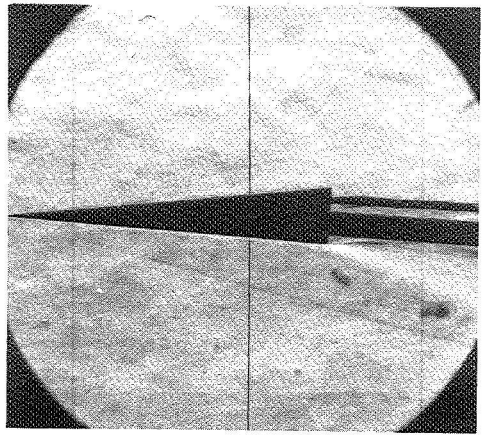

Jet off

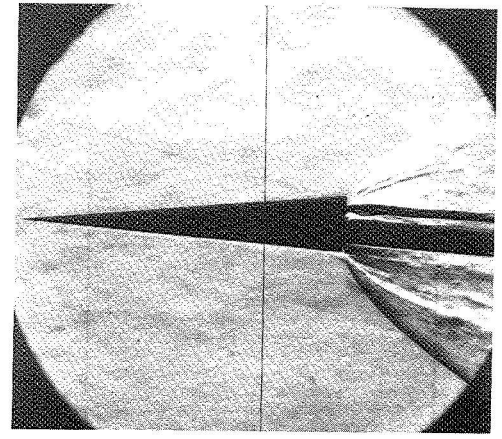

p_j/p_∞=842

M_∞=4.00

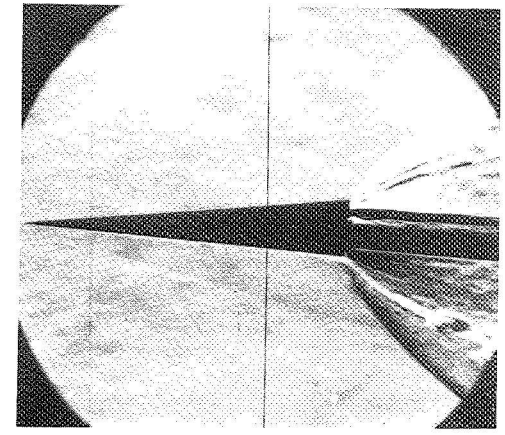

p_j/p_∞=1387

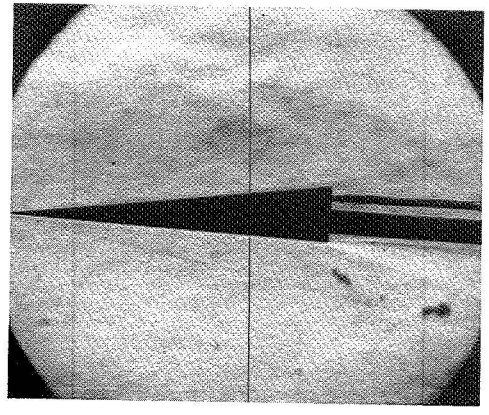

Jet off

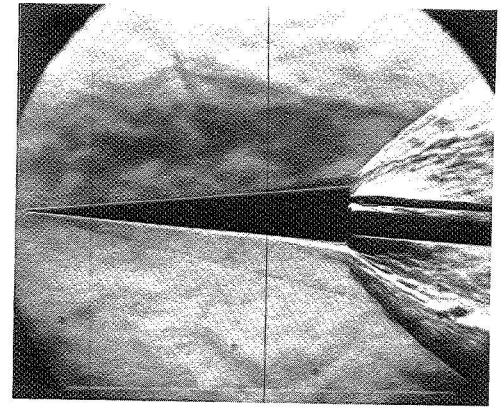

p_j/p_∞=1833

M_∞=5.00

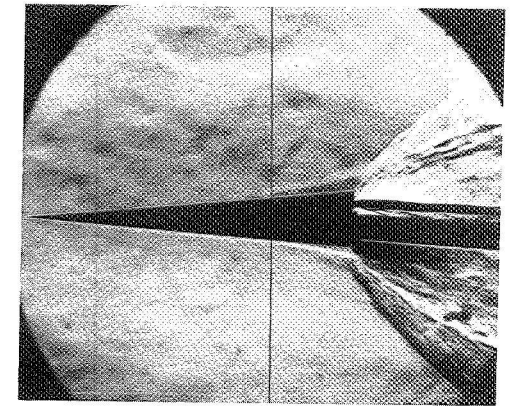

p_j/p_∞=2722

(g) M_∞ = 4.00 and 5.00; $\alpha = 5^0$.

L-70-1520

Figure 5.- Continued.

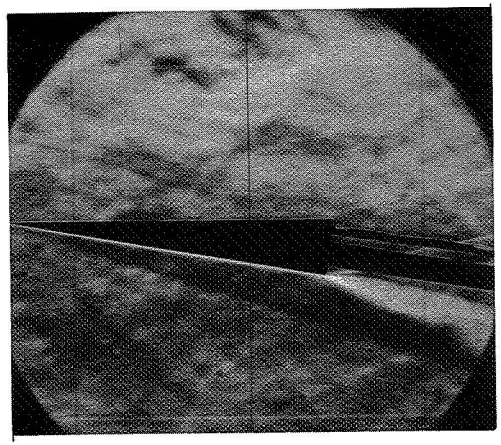

Jet off

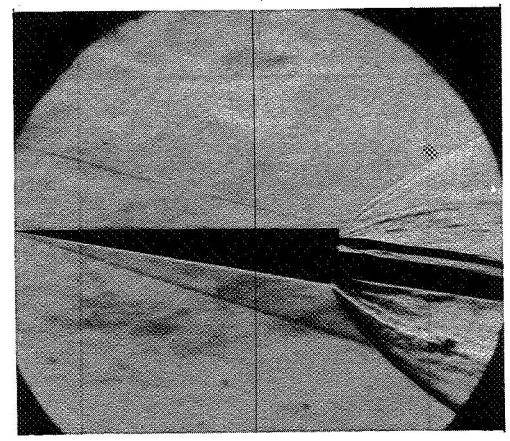

p_j/p_∞=656

M_∞=4.00

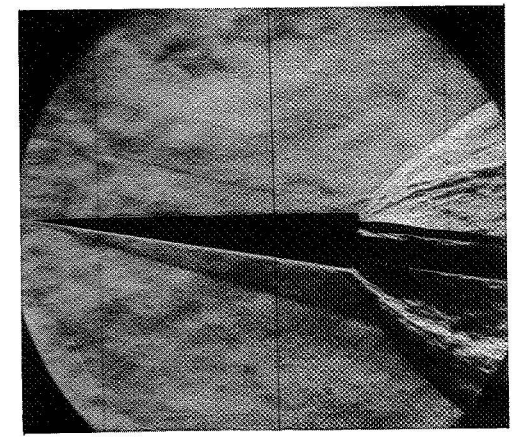

p_j/p_∞=1372

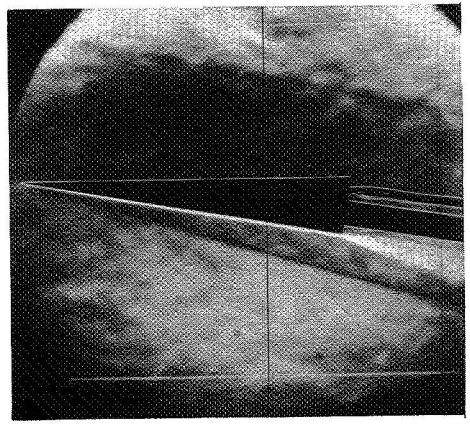

Jet off

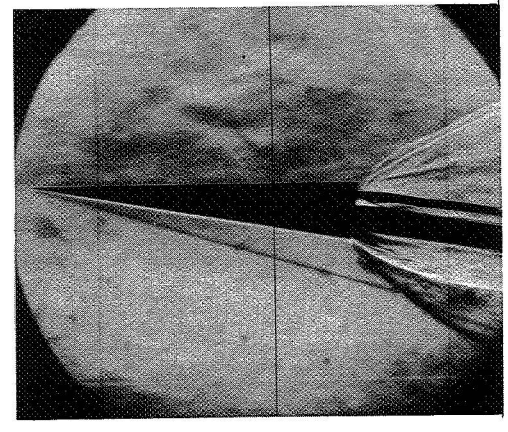

p_j/p_∞=563

M_∞=5.00

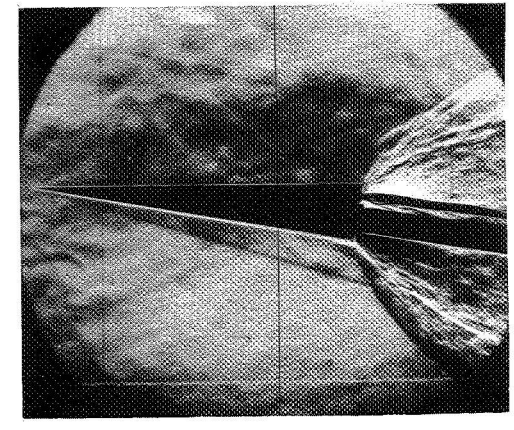

p_j/p_∞=2704

(h) M_∞ = 4.00 and 5.00; α = 10°.

L-70-1519

Figure 5.- Concluded.

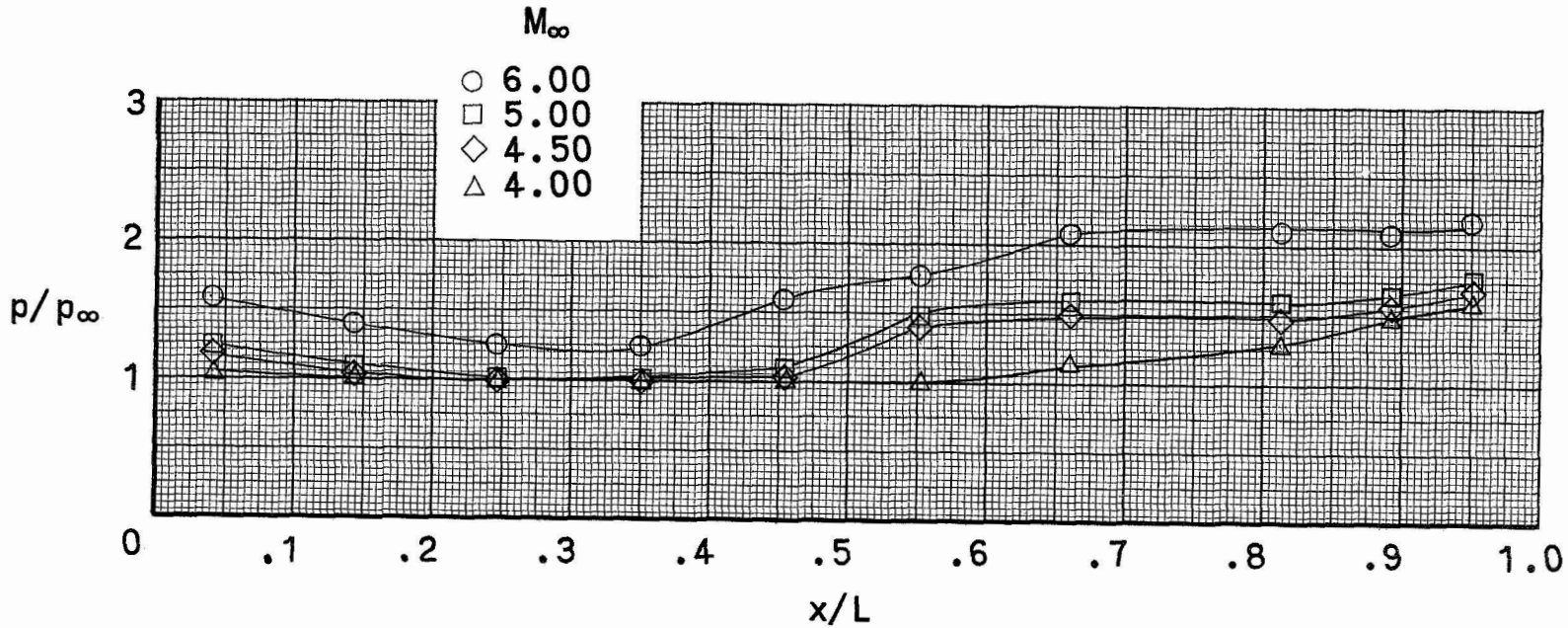

Figure 6.- Effect of Mach number on the model pressure distribution for $p_j/p_\infty \approx 1300$. $\alpha = 0^0$.

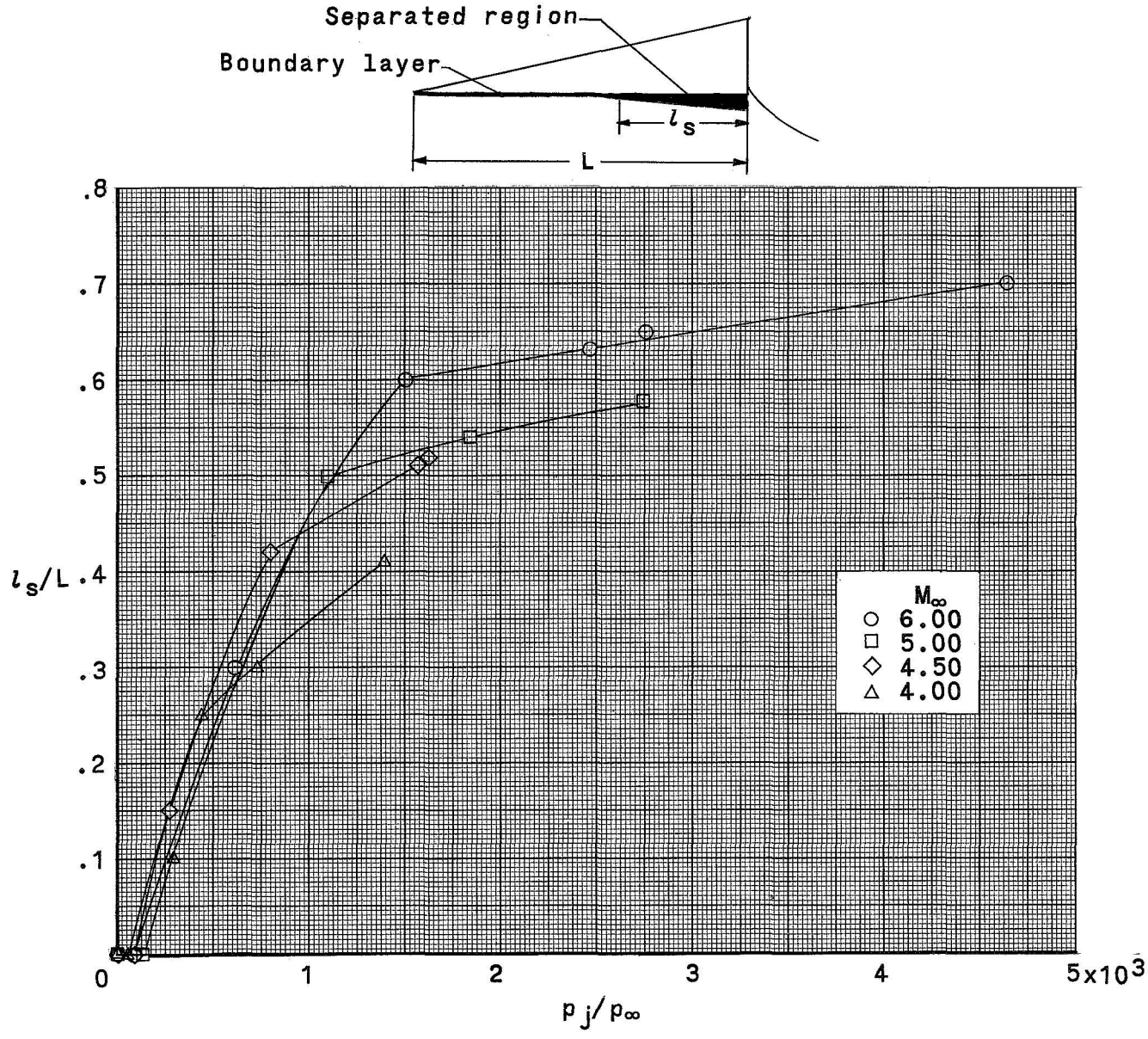

Figure 7.- Effect of Mach number on the length of separated flow region at $\alpha = 0^0$.

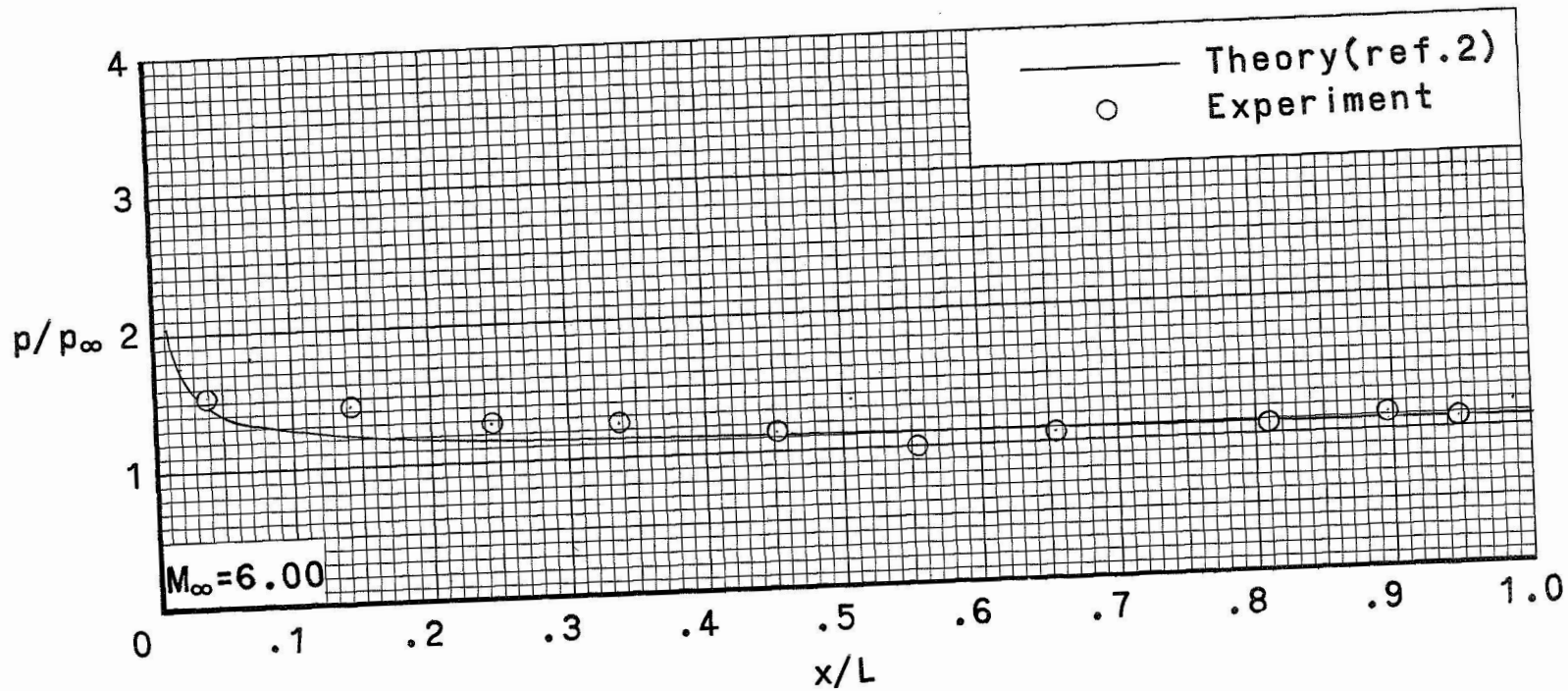

Figure 8.- Comparison of model pressure distribution with theory for jet-off conditions. $p_j/p_\infty = 0$; $\alpha = 0^o$.

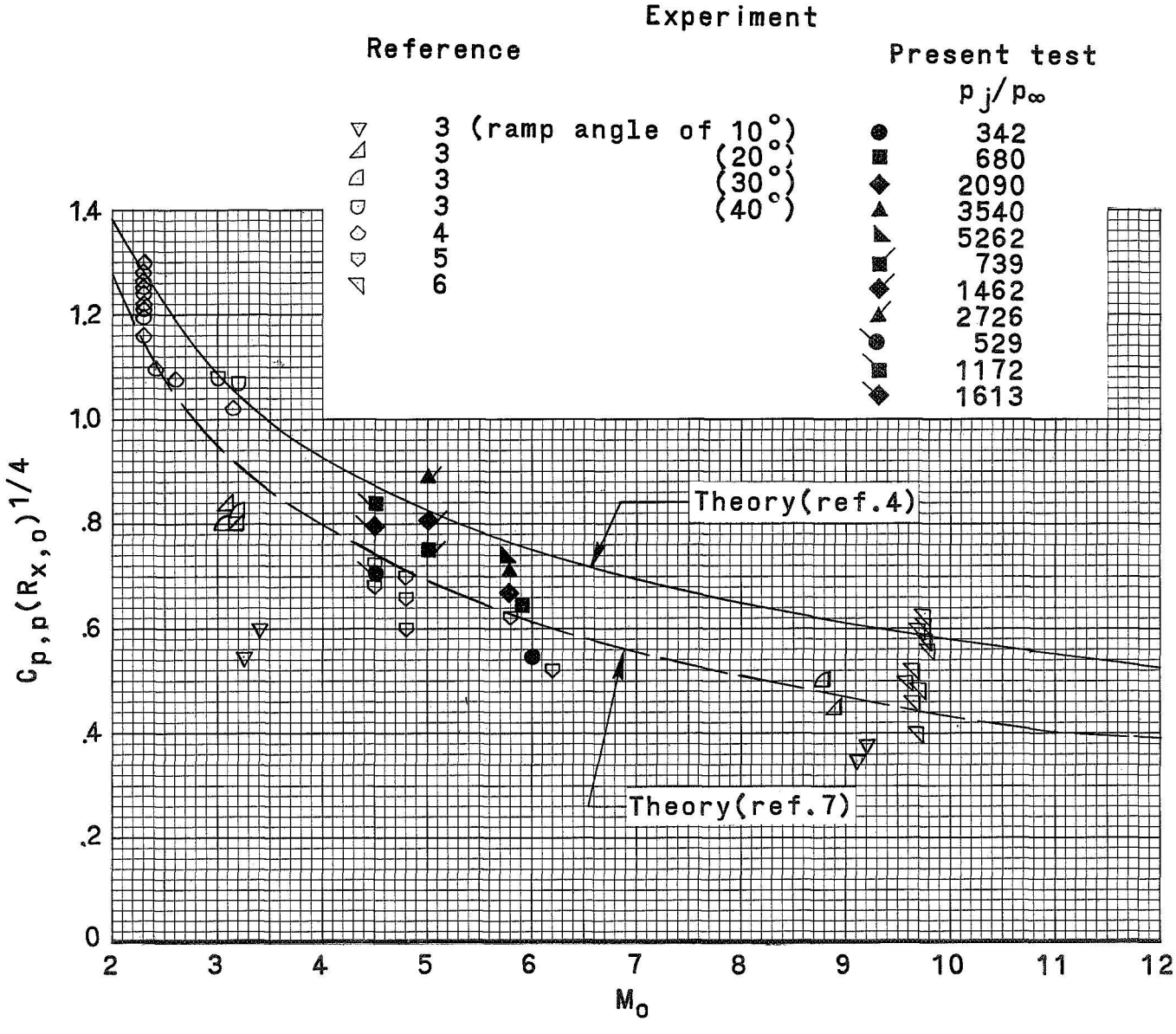

Figure 9.- Correlation of the plateau pressure coefficient. $\alpha = 0^0$.

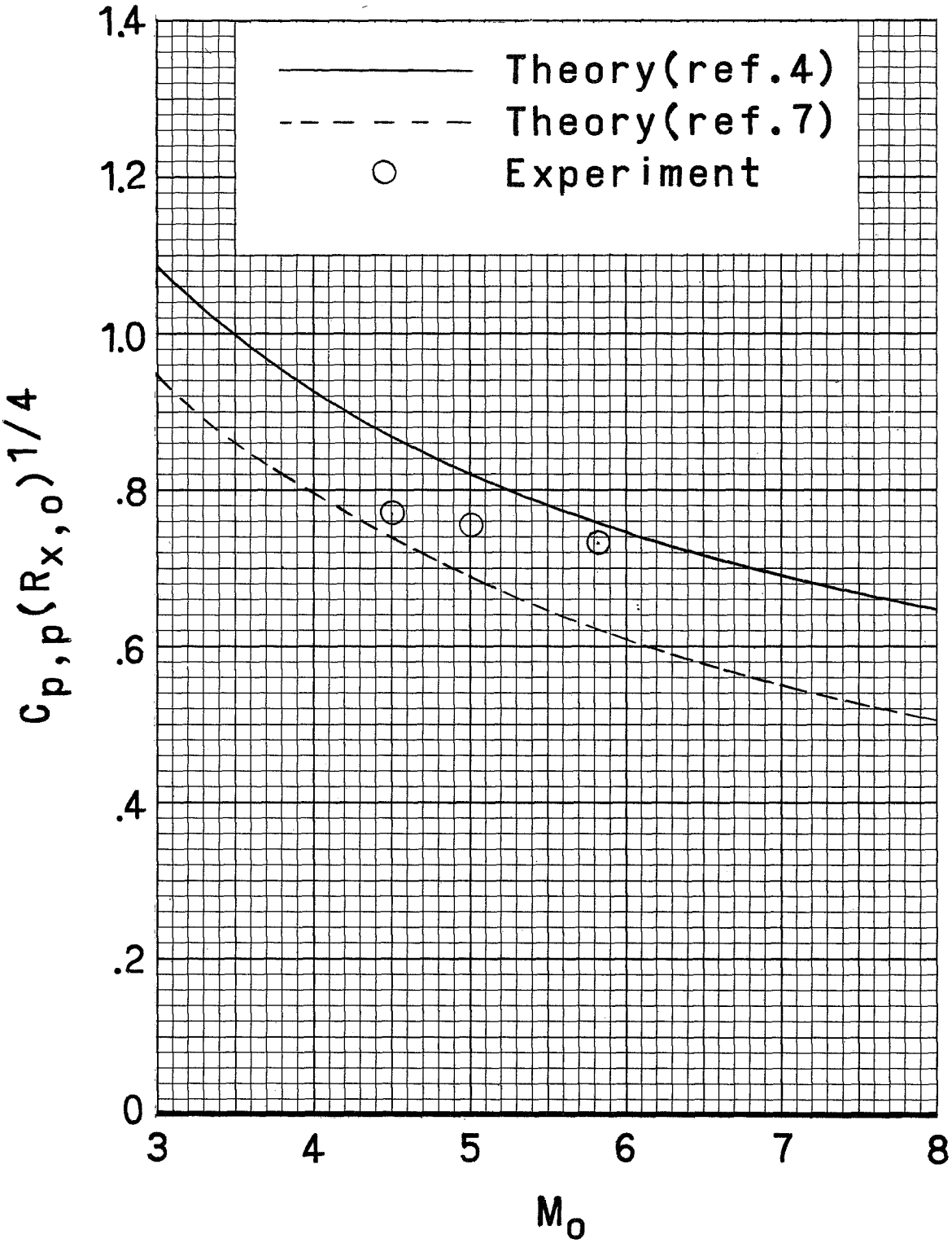

Figure 10.- Correlation of the plateau pressure coefficient at a constant plume shape. $p_j/p_\infty \approx 1300$; $\alpha = 0^0$.

NASA-Langley, 1970 —— 1 L-6980

NATIONAL AERONAUTICS AND SPACE ADMINISTRATION
WASHINGTON, D.C. 20546

OFFICIAL BUSINESS

FIRST CLASS MAIL

POSTAGE AND FEES PAID
NATIONAL AERONAUTICS AN
SPACE ADMINISTRATION

POSTMASTER: If Undeliverable (Section 158
Postal Manual) Do Not Retur

"The aeronautical and space activities of the United States shall be conducted so as to contribute . . . to the expansion of human knowledge of phenomena in the atmosphere and space. The Administration shall provide for the widest practicable and appropriate dissemination of information concerning its activities and the results thereof."

—NATIONAL AERONAUTICS AND SPACE ACT OF 1958

NASA SCIENTIFIC AND TECHNICAL PUBLICATIONS

TECHNICAL REPORTS: Scientific and technical information considered important, complete, and a lasting contribution to existing knowledge.

TECHNICAL NOTES: Information less broad in scope but nevertheless of importance as a contribution to existing knowledge.

TECHNICAL MEMORANDUMS: Information receiving limited distribution because of preliminary data, security classification, or other reasons.

CONTRACTOR REPORTS: Scientific and technical information generated under a NASA contract or grant and considered an important contribution to existing knowledge.

TECHNICAL TRANSLATIONS: Information published in a foreign language considered to merit NASA distribution in English.

SPECIAL PUBLICATIONS: Information derived from or of value to NASA activities. Publications include conference proceedings, monographs, data compilations, handbooks, sourcebooks, and special bibliographies.

TECHNOLOGY UTILIZATION PUBLICATIONS: Information on technology used by NASA that may be of particular interest in commercial and other non-aerospace applications. Publications include Tech Briefs, Technology Utilization Reports and Notes, and Technology Surveys.

Details on the availability of these publications may be obtained from:

SCIENTIFIC AND TECHNICAL INFORMATION DIVISION

NATIONAL AERONAUTICS AND SPACE ADMINISTRATION

Washington, D.C. 20546